Power and Frequency Control of Active Generator used for Smart Grid Applications

Ehsan Limouchi[1], Seyed Abbas Taher[2], Babak Ganji[3*]
1- Department of Electrical and Computer Engineering, University of Kashan, Kashan, Iran.
Email: ehsan.limuchi@gmail.com
2- Department of Electrical and Computer Engineering, University of Kashan, Kashan, Iran.
Email: sataher@kashanu.ac.ir
3- Department of Electrical and Computer Engineering, University of Kashan, Kashan, Iran.
Email: bganji@kashanu.ac.ir (Corresponding author)

Received: May 2019 Revised: August 2019 Accepted: September 2019

ABSTRACT:
Nowadays, renewable energy sources such as photovoltaic and active generators are utilized frequently in modern power systems especially micro-grid. By providing electrical energy using micro-grid systems, the reliability and quality of the system can be improved. A micro-grid connected to the network depends on the main grid and consequently assessing the power quality during independent functioning (islanded mode) is important. The aim of the present work is to perform active, reactive power distribution strategies (control) for active generators used in smart grids. The proposed control method is the sliding mode which controls the active as well as reactive power and frequency. Here, based on sliding mode control method, droop control is developed for active generator. This controller is simulated for active generator by MATLAB/SIMULINK and simulation results are given. Based on the obtained simulation results, efficiency of sliding mode in regulating active and reactive power and controlling domain voltage and frequency are shown.

KEYWORDS: Active Generators, Sliding Mode Controller, Micro-grid, Voltage Source Converter, Space Vector Pulse Width Modulation.

1. INTRODUCTION

One of the most significant features of a micro-grid is its capacity for independent functioning and islanding. This characteristic results in reliability and enhanced quality of subscribers' power located in the micro-grid. Once separated from the power system, duties and function modes of the available sources in the micro-grid are changed. When connected to the network, all these duties are resolved and resources produce a pre-identified level of active power [1-3]. In power systems, constancy of voltage and frequency is very important. Frequently, the power converter interface from the DC source to the grid consists of a current controlled Voltage Source Converter (VSC). The classic control method for the grid-connected VSC is usually based on grid-voltage or virtual-flux oriented vector control schemes [4-6]. The power systems are known as non-linear dynamic systems and regarding their development and evolution, their endurance is of great significance. Meanwhile, the characteristics of the current power systems have the complicated endurance issues and they result in unstable system [7]. However, recent developments in control systems and protection systems have made it possible to know and analyze all aspects of the endurance. The voltage instability usually occurs when the transfer capacity of power system is reduced due to a fault and while it is exposed to energy saving systems such as battery. Many sustainable energy sources such as photovoltaic systems are DC and an active generator can be considered as a distributed power source which is connected to the micro-grid [8]. Different control methods have been used so far to connect active generator to the network in order to have access to correct functioning as well as appropriate power distribution and boosting stability.

Recently, various methods to control output power of the inverter along with controlling and managing power are proposed. Researchers have worked on the designing of the controller. Among which are Proportional Integrate (PI) control [9-10], resonance proportional control [11-12], Fuzzy control [13-14] and predicted control [15-16]. The classic PI is a simple controller with easy performance. However, it has permanent mistake in following current signal and it is sensitive to changing systems' parameters. In addition,

regulating PI is complex. A way to control active power of the generator is to control it by sliding mode controller. In comparison to PI control, it has higher speed. Moreover, sliding mode control is a robust method which is effective in uncertainty and external disturbances [17-20]. In [21], a robust second order sliding mode control is proposed for voltage regulation in a DC micro grid with unknown load demand and modelling uncertainties. A new fuzzy sliding mode droop control is also introduced in [22] for power sharing among multiple islanded DC DGs. As micro-grids are islanding when controlling voltage-frequency, they need suitable control structure to achieve aims such as controlling voltage and frequency in valid domain [23-24]. In addition, the purpose to reduce THD is the form of output voltage. Defining a good level for appropriate switching for setting guarantee to follow reference signal with total harmonic distortion is very important.

Due to its strength against uncertainties of the model and external disturbances and its simplicity in performance, sliding mode control method is an effective method for controlling voltage and frequency in a micro-grid system. In the present study, switching with constant frequency by sliding mode control for an active generator is examined. However, direct use of sliding mode control is not easily possible because of chattering phenomenon for controlling switching [25-26]. Accordingly, Space Vector Pulse Width Modulation (SVPWM) is used to relax controlling rules and therefore fluctuations with high frequencies are omitted as much as possible in the outlet [27-29]. Control of active generator is presented here for providing reactive and active power in the grid and controlling voltage and frequency. In the present paper, a new sliding mode control of SVPWM switching method is proposed to adjust active and reactive power generation of an active generator for an islanded smart grid application. Controlling the power of a reference active generator is done by sliding mode while it is connected to distribution network. By selecting sliding mode control, a fast and stable control method for controlling active generator is obtained to increase the power system stability and reliability. The present study is composed of the following parts. In section 2, mathematical formula and modeling of active generator are introduced. The proposed sliding mode control method and its details are presented in section 3. In section 4, simulation results are presented, and finally the paper is concluded in the section 5.

2. THE MODELLING PROPOSED FOR ACTIVE GENERATOR

When different generators are working in parallel mode depicted in Fig. 1, each generator can automatically change the power level. This is profitable as generators change active power by considering frequency changes as the input signal and the function of performance are reduced by calculating power. The results of increasing load in the reduction of the system frequency and consequently generators would increase their power level according to the graph of the voltage reduction. In this case, the frequency of the system would increase again.

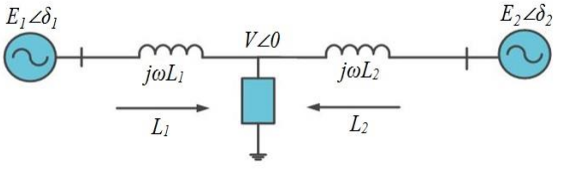

Fig. 1. The parallel operation of power generators.

The frequency droop is defined as follows:

$$f = f_0 + k_P(P - P_0), \qquad k_p = \frac{\Delta f}{\Delta p} \tag{1}$$

Where, Δf is change of frequency from normal frequency and ΔP is change of power from set point. A typical frequency droop value (k_P) for grid scale synchronous generator is assumed to be 5 %. Changing reactive power means variations of the voltage of coupling point. This can be achieved by changing the excitation of the generator. The relationship of this droop behavior can be shown simply as follows:

$$V = V_{grid} + k_q(Q - Q_0) \tag{2}$$

The frequency droop characteristic defined at above can be interpreted as follows. When frequency falls from rated f_0 to f, the power output of the generating unit is allowed to increase the power dispatching value from P_0 to P. A falling frequency indicates an increase in loading and a requirement for more active power. In the same way, when the coupling point voltage of synchronous generator decreases from V_{grid} to V, generators are allowed to increase its reactive power from Q_0 to Q level. In the case that two generators provide the power to a load, the active and reactive power sharing between each generator depends on load angle and magnitude of voltage deference, respectively. The schematic of the proposed droop control method is shown in Fig. 2.

To obtain a control capability independent from active and reactive power in VCS, it is necessary to obtain two control variables for each. Changing dq can be used for the two independence current variables: current i_d for control of real power and current i_q for controlling reactive power. According to Fig. 3, converting three-phase voltages/currents to dq system

with two turning axis consists of two converting stages including Clark and Park transformation.

The Clark transformation helps us to transform three-phase voltage/current sequence (v_{abc}/I_{abc}) to stationary voltage/current reference frame ($v_{\alpha\beta}/I_{\alpha\beta}$). This process can be shown as following:

$$\begin{bmatrix} v_\alpha \\ v_\beta \end{bmatrix} = \frac{2}{3}\begin{bmatrix} 1 & -\frac{1}{2} & -\frac{1}{2} \\ 0 & \frac{\sqrt{3}}{2} & -\frac{\sqrt{3}}{2} \end{bmatrix}\begin{bmatrix} v_a \\ v_b \\ v_c \end{bmatrix} \quad (3)$$

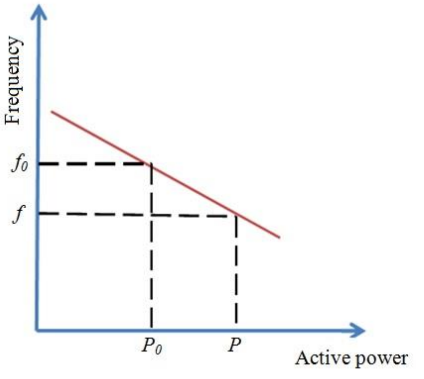

(a)

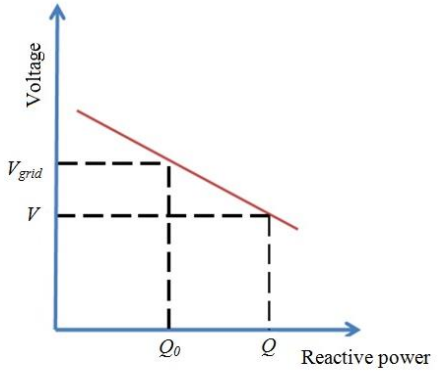

(b)

Fig. 2. Droop control method: (a) frequency droop, (b) voltage droop.

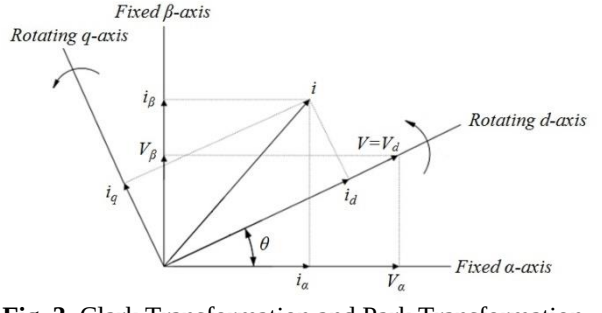

Fig. 3. Clark Transformation and Park Transformation.

Similarly, the Park transformation is used to transform stationary voltage/current reference frame to a rotating voltage/current reference frame using below equation:

$$\begin{bmatrix} v_d \\ v_q \end{bmatrix} = \begin{bmatrix} \cos\theta & \sin\theta \\ -\sin\theta & \cos\theta \end{bmatrix}\begin{bmatrix} v_\alpha \\ v_\beta \end{bmatrix} \quad (4)$$

Moreover, a symmetrical three-phase system is supposed here in which $v_a=V\cos\theta$, $v_b=V\cos(\theta-2\pi/3)$ and $v_c=V\cos(\theta+2\pi/3)$. By applying Clark transformation and park transformation, we have:

$$\begin{bmatrix} v_\alpha \\ v_\beta \end{bmatrix} = \frac{2}{3}\begin{bmatrix} V\cos\theta \\ V\sin\theta \end{bmatrix}\begin{bmatrix} v_d \\ v_q \end{bmatrix} = \begin{bmatrix} v \\ 0 \end{bmatrix} \quad (5)$$

A three-phase VSC system is considered where, DC power is converted to AC and it is then transferred to infinite AC-bus. Each IGBT transistor is controlled by a PWM system to generate the required AC waveform. The voltage balance equation for the above-mentioned system can be written as:

$$v_{abc,conv} = v_{abc} + Ri_{abc} + L\frac{di_{abc}}{dt} \quad (6)$$

$$\begin{bmatrix} v_{a,conv} \\ v_{b,conv} \\ v_{c,conv} \end{bmatrix} = \begin{bmatrix} v_a \\ v_b \\ v_c \end{bmatrix} + R\begin{bmatrix} i_a \\ i_b \\ i_c \end{bmatrix} + L\frac{d}{dt}\begin{bmatrix} i_a \\ i_b \\ i_c \end{bmatrix} \quad (7)$$

Taking dq transformation, the following equations are resulted:

$$\begin{bmatrix} v_{dconv} \\ v_{qconv} \end{bmatrix} = \begin{bmatrix} v_d \\ v_q \end{bmatrix} + R\begin{bmatrix} i_d \\ i_q \end{bmatrix} + L\frac{d}{dt}\begin{bmatrix} i_d \\ i_q \end{bmatrix} + L\begin{bmatrix} 0 & -\omega \\ \omega & 0 \end{bmatrix}\begin{bmatrix} i_d \\ i_q \end{bmatrix} \quad (8)$$

$$v_{d,conv} = v_d + Ri_d + L\frac{di_d}{dt} - \omega Li_q \quad (9)$$

$$v_{q,conv} = v_q + Ri_q + L\frac{di_q}{dt} + \omega Li_d \quad (10)$$

And, for DC-bus side:

$$I_L = c\frac{dv_{dc}}{dt} + I_{dc} \quad (11)$$

The power balance equation is given by:

$$\frac{3}{2}\left(v_d i_d + v_q i_q\right) = V_{dc} I_{dc} \quad (12)$$

Considering grid voltage along with d-axis (grid voltage=v_d and v_q=0), instantaneous active and reactive powers are calculated using below equations:

$$p=\frac{3}{2}v_d i_d \quad (13)$$

$$q=-\frac{3}{2}v_d i_q \quad (14)$$

This means that the active and reactive powers can be controlled independently with i_d and i_q current components. The basic active generator system is illustrated in Fig. 5.

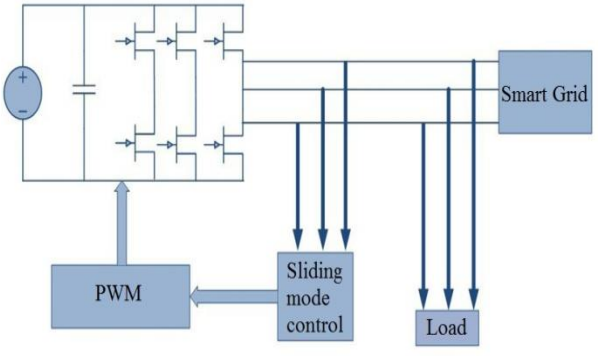

Fig. 4. Basic active generator system.

2.1. The Model used for Inverter

The considered power inverter systems depicted in Fig. 5 consist of usual VSC, and LC filter, ΔY transformation unit, and controlling systems. The main parts of the Microgrid are described in the following:

1) Three-phase bridge and PWM: It is the main inverter which is controlled to reach active and reactive power in two ways based on PWM.
2) PLL and coordination unit: PLL is used for receiving frequency, the current voltage and the data of phase angle.
3) LC filter: It is utilized to reduce the uniformity of the output wave.
4) Δy transformation and connection grid: It is for changing levels voltage.
5) DC source: It is required to provide needed power of the system
6) Sliding mode controlling system: It is used to control dispatching active and reactive power, set voltage and frequency.

By using i_d and i_q which are derived from the measured I_{abc}, V_{abc}, the VSC controlling system produces SVPWM signal needed for inverting and it consists of the following parts:

1) The sub-system for measuring PLL
2) Current controller
3) The producer of the width of pulse PWM

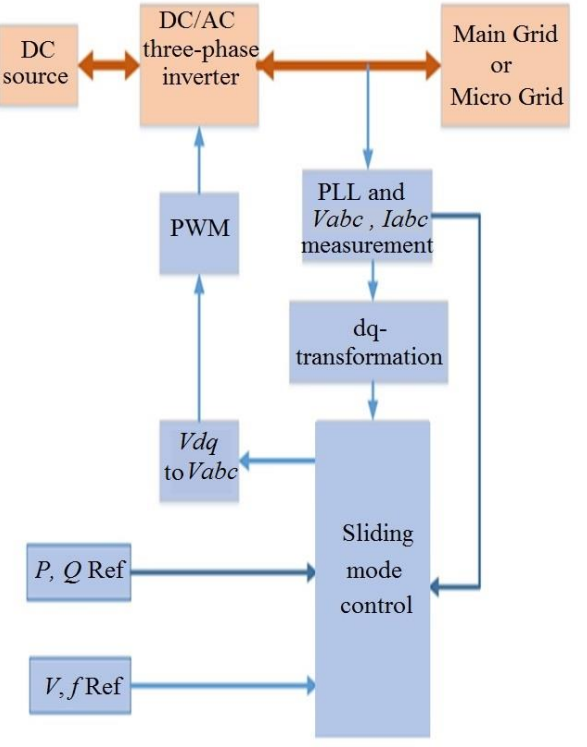

Fig. 5. Active generator with sliding mode control.

3. SLIDING MODE CONTROL

In order to perform sliding mode control, convertor functions are written in stationary mood as follows.

$$v_{\alpha,conv} = v_\alpha + Ri_\alpha + L\frac{di_\alpha}{dt} \quad (15)$$

$$v_{\beta,conv} = v_\beta + Ri_\beta + L\frac{di_\beta}{dt} \quad (16)$$

Choosing the sliding level based on the error of active and reactive power, we have:

$$s=\begin{bmatrix} s_P \\ s_Q \end{bmatrix} \quad (17)$$

$$s_p = e_p(t)+k_p\int e_p\,dt+e_p(0) \quad (18)$$

$$s_Q = e_Q(t)+k_Q\int e_Q\,dt+e_Q(0) \quad (19)$$

$$e_p = P^*-P \quad (20)$$

$$e_Q = Q^*-Q \quad (21)$$

When variables reach to the surface, the following conditions should be provided to remain on the surface:

$$s_P = s_Q = \frac{ds_P}{dt} = \frac{ds_Q}{dt} = 0 \quad (22)$$

$$\frac{ds_P}{dt} = \frac{de_P}{dt} + k_p e_p = -\frac{d}{dt}P + K_p\left(P^*-P\right) \quad (23)$$

$$\frac{ds_Q}{dt}=\frac{de_Q}{dt}+k_Q e_Q=-\frac{d}{dt}Q+K_Q\left(Q^*-Q\right) \tag{24}$$

$$P=1.5\left(v_\alpha i_\alpha+v_\beta i_\beta\right) \tag{25}$$

$$Q=1.5\left(v_\beta i_\alpha+v_\alpha i_\beta\right) \tag{26}$$

$$\frac{dp}{dt}=1\cdot5\left(v_\alpha\frac{di_\alpha}{dt}+i_\alpha\frac{dv_\alpha}{dt}+v_\beta\frac{di_\beta}{dt}+i_\beta\frac{dv_\beta}{dt}\right) \tag{27}$$

$$\frac{dQ}{dt}=1\cdot5\left(v_\beta\frac{di_\alpha}{dt}+i_\alpha\frac{dv_\beta}{dt}-v_\alpha\frac{di_\beta}{dt}-i_\beta\frac{dv_\alpha}{dt}\right) \tag{28}$$

The voltage and current waveforms are supposed to be ideal:

$$v_\alpha=V\sin(\omega t) \tag{29}$$

$$v_\beta=V\sin\left(\omega t-\frac{\pi}{2}\right)=-V\cos(\omega t) \tag{30}$$

Thus,

$$\frac{dv_\alpha}{dt}=\omega V\cos(\omega t)=-\omega v_\beta \tag{31}$$

$$\frac{dv_\beta}{dt}=\omega V\sin(\omega t)=-\omega v_\alpha \tag{32}$$

From (15) and (16), we have:

$$\frac{di_\alpha}{dt}=\frac{1}{L}\left(v_{\alpha,conv}-v_\alpha-Ri_\alpha\right) \tag{33}$$

$$\frac{di_\beta}{dt}=\frac{1}{L}\left(v_{\beta,conv}-v_\beta-Ri_\beta\right) \tag{34}$$

By substituting (15) and (16) into (27) and (28):

$$\begin{aligned}\frac{dP}{dt}=&-1.5\frac{R}{L}\left(v_\alpha i_\alpha+v_\beta i_\beta\right)-\frac{1.5}{L}\left(v_\alpha^2+v_\beta^2\right)\\&-1.5\omega_i\left(v_\beta i_\alpha-v_\alpha i_\beta\right)+\frac{1.5}{L}\left(v_\alpha v_{\alpha,conv}+v_\beta v_{\beta,conv}\right)\end{aligned} \tag{35}$$

$$\begin{aligned}\frac{dQ}{dt}=&-1.5\omega\left(v_\alpha i_\alpha-v_\beta i_\beta\right)-\frac{1.5R}{L}\left(v_\beta i_\alpha-v_\alpha i_\beta\right)\\&+\frac{1.5}{L}\left(v_\beta v_{\alpha,conv}-v_\alpha v_{\beta,conv}\right)\end{aligned} \tag{36}$$

And:

$$\begin{aligned}\frac{dP}{dt}=&-\frac{R}{L}P-\omega Q-\frac{1.5}{L}\left(v_\alpha^2+v_\beta^2\right)\\&+\frac{1.5}{L}\left(v_\alpha v_{\alpha,conv}+v_\beta v_{\beta,conv}\right)\end{aligned} \tag{37}$$

$$\frac{dQ}{dt}=-\omega P-\frac{R}{L}Q-\frac{1.5}{L}\left(v_\beta v_{\alpha,conv}-v_\alpha v_{\beta,conv}\right) \tag{38}$$

$$\begin{aligned}\frac{d}{dt}\begin{bmatrix}P\\Q\end{bmatrix}=&\frac{1\cdot5}{L}\begin{bmatrix}v_\alpha & V_\beta\\V_\beta & -V_\alpha\end{bmatrix}\begin{bmatrix}v_{\alpha,conv}\\v_{\beta,conv}\end{bmatrix}\\&+\begin{bmatrix}-\frac{R}{L} & -\omega\\\omega & -\frac{R}{L}\end{bmatrix}\begin{bmatrix}P\\Q\end{bmatrix}-\frac{1\cdot5}{L}\begin{bmatrix}v_\alpha{}^2+v_\beta{}^2\\0\end{bmatrix}\end{aligned} \tag{39}$$

By substituting (39) in (23) and (24), we have:

$$\frac{ds}{dt}=F+Du_{conv_{\alpha\beta}} \tag{40}$$

Where,

$$\begin{aligned}&F=\begin{bmatrix}F_1 & F_2\end{bmatrix}^T;\ u_{conv_{\alpha\beta}}=\begin{bmatrix}v_{\alpha,conv} & v_{\beta,conv}\end{bmatrix}^T\\&\begin{bmatrix}F_1\\F_2\end{bmatrix}=+\begin{bmatrix}\frac{R}{L} & \omega\\-\omega & \frac{R}{L}\end{bmatrix}\begin{bmatrix}P\\Q\end{bmatrix}-\frac{1\cdot5}{L}\begin{bmatrix}v_\alpha{}^2+v_\beta{}^2\\0\end{bmatrix}\\&\qquad+\begin{bmatrix}K_p\left(P^*-P\right)\\K_Q\left(Q^*-Q\right)\end{bmatrix}\\&D=\frac{1\cdot5}{L}\begin{bmatrix}v_\alpha & v_\beta\\v_\beta & -v_\alpha\end{bmatrix}\end{aligned} \tag{41}$$

The Lyapunov function is selected as follows:

$$W=\frac{1}{2}S^TS\geq0 \tag{42}$$

Calculating the derivation of the Lyapunov function results in:

$$\begin{aligned}\frac{dW}{dt}=&\frac{1}{2}\left(S^T\frac{ds}{dt}+S\frac{ds^T}{dt}\right)=S^T\frac{ds}{dt}\\&=S^T\left(F+Du_{conv_{\alpha\beta}}\right)\end{aligned} \tag{43}$$

The rule of switching should be chosen as the derivation of W is definitely negative:

$$\begin{bmatrix}v_{\alpha,conv}\\v_{\beta,\ conv}\end{bmatrix}=-D^{-1}\left\{\begin{bmatrix}F_1\\F_2\end{bmatrix}+\begin{bmatrix}K_{P1} & 0\\0 & K_{Q1}\end{bmatrix}\begin{bmatrix}sgn(S_P)\\sgn(S_Q)\end{bmatrix}\right\} \tag{44}$$

Where:

$$sgn(s_j)=\begin{cases}1 & \text{if } s_j>0\\-1 & \text{if } s_j<0\end{cases} \tag{45}$$

And for proving the stability:

$$\begin{aligned}\frac{dW}{dt}&=S^T\frac{ds}{dt}=-S^T\begin{bmatrix}K_{P_1} & 0\\ 0 & K_{Q_1}\end{bmatrix}\begin{bmatrix}sgn(S_P)\\ sgn(S_Q)\end{bmatrix}\\ &=-K_{P_1}S_P\,sgn(S_P)-K_{Q_1}S_Q\,sgn(S_Q)\\ &=-K_{P_1}\,|S_P|-K_{Q_1}\,|S_Q|<0\end{aligned} \tag{45}$$

As a result, the derivation of the Lyapunov function is definitely negative which results in tangent constancy of control system. To prove the robust of control system disturbance, we have:

$$H=[H_1 \quad H_2]^T \tag{46}$$

Then, (40) can be rewritten as follows:

$$\frac{ds}{dt}=F+Du_{conv_{\alpha\beta}}+H \tag{47}$$

And (42) is rewritten as:

$$\frac{dW}{dt}=+S^T\frac{ds}{dt}=S^T\left\{\begin{bmatrix}H_1\\ H_2\end{bmatrix}-\begin{bmatrix}K_{P_1} & 0\\ 0 & K_{Q_1}\end{bmatrix}\begin{bmatrix}sgn(S_P)\\ sgn(S_Q)\end{bmatrix}\right\} \tag{48}$$

By correct selection of $K_{P_1} > |H_1|$, $K_{Q_1} > |H_2|$, integration of the Lyapunov function is definitely negative and consequently the considered control system is robust. To face chattering phenomenon in the sliding mode control, saturation is used instead of sign as follows:

$$\text{sat(s)}=\begin{cases}1 & \text{if } s>\lambda\\ \dfrac{s}{\lambda} & \text{if } |s|\leq\lambda\\ -1 & \text{if } |s|<-\lambda\end{cases} \tag{49}$$

Where, λ is the border layer of sat.

Finally, the voltage is connected to the grid's frame:

$$v_{conv_{\alpha\beta}}=v_{dq}e^{-J\theta} \tag{50}$$

4. SIMULATION RESULTS

A typical test system has been established consisting of an active generator and a transmission system which is shown in Fig. 6. The system parameters are summarized in Table 1. In the previous sections, the mathematical formula for active generators and sliding mode control were introduced. The active generator and the convertor are simulated in MATLABL/SIMULINK and the related simulation results are presented here. In addition, the proposed sliding mode control method is compared to PI classic controller.

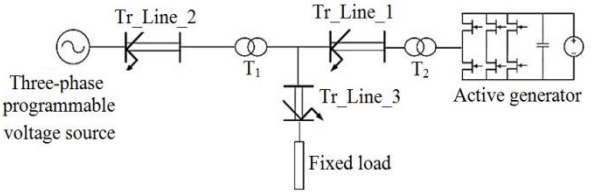

Fig. 6. Simulation model of the active generator, load and grid.

To evaluate performance of the proposed sliding mode control method, comparative simulations involving PI strategy described in [8] are also presented under the same conditions. In addition, the ability of LVRT (Low Voltage Ride Through) and reactive power support are investigated. The active generator response during voltage dip and active power step for the proposed sliding mode control and PI are compared in Fig. 7. The waveforms shown in this figure illustrate frequency, active power, reactive power and phase current of active-generator. Initially, voltage frequency and amplitude references are set to 50 Hz and 1 pu, respectively. The grid voltage dips from 1 pu to 0.7 pu symmetrically (30% depth), starts at t=0, and lasts for 0.3 sec. The inerter active and reactive power references are varied respect to voltage frequency and amplitude variations as shown in Fig. 7. The voltage and frequency are controlled by adjusting active and reactive power generation. The transient responses of active and reactive power for two mentioned methods are given in Table 2. It is evident that time-response of reactive and active power of the proposed sliding mode control is much faster than the PI.

According to Fig. 7 and Table 2, the proposed sliding mode control has current Total Harmonics Distortion (THD) similar to that of PI control and their steady-state behaviors are the same. Moreover, proposed sliding mode control tracks variation of active power reference better than PI control. Thus, the proposed sliding mode control can adjust frequency and amplitude of voltage better and faster than PI control, and therefore the proposed sliding mode control has better LVRT capability. Due to high speed of the proposed control method, better conditions will be provided for the power network from voltage and frequency stability point of view. At t = 0.3 sec, voltage drop is cleared and the proposed sliding mode control tracks new active and reactive powers references as observed in Fig. 7. The active power is stepped from 0.97 pu to 0.75 *pu* at t = 0.7 *s*, while the reactive power is kept constant. Based on the obtained simulation results, it is seen that steady state performance of the proposed sliding mode control is similar to PI, while its transient response is much faster. The aforementioned comparative advancements show the accuracy and effectiveness of the proposed method during transient and steady-state conditions accordingly.

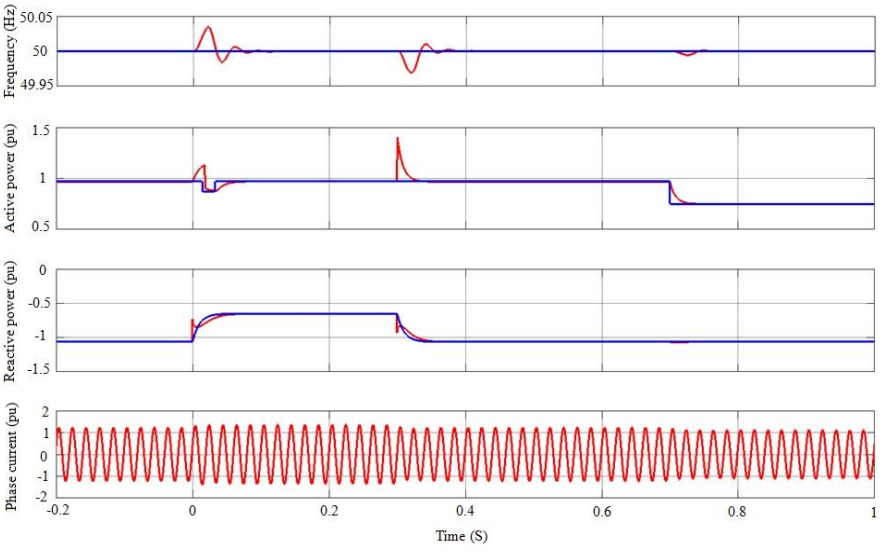

(a)

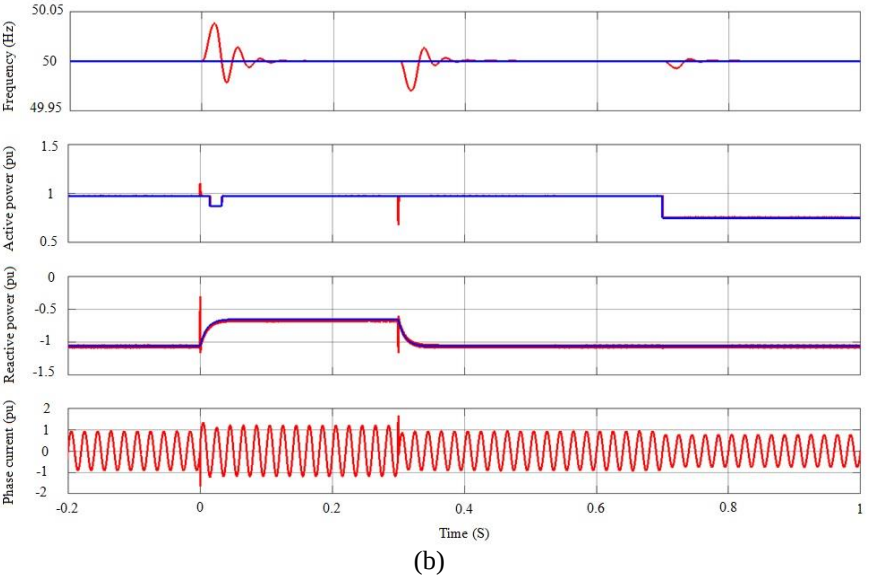

(b)

Fig. 7. Frequency, active and reactive power and phase current: (a) PI control, (b) proposed SMC method.

Table 1. The system parameters.

Parameter	Value
Voltage	11 kV
Frequency	50 Hz
Active power	1 MW
Reactive power	1 MVAR
Tr_line1	3 km
Tr_line2	3 km
Tr_line3	1 km

To evaluate the robustness of the proposed sliding mode control strategy against system parameters variations, more tests are carried out and the related simulation results are presented in Fig. 8. The parameters variations can occur due to possible temperature variation, skin effect, etc. The test results are compared in this figure when values of transmission line resistances applied in the control system are varied by +50%. The step change in active power is applied: active power reference is changed from 0.9 to 0.75 *pu* at t = 0 sec and then backed to 0.9 *pu* at t = 0.2 sec. With regard to Fig. 8, these parameters variations have insignificant influence on system performance and the system maintains superb performance even with such large errors in the resistances. In addition, it is seen that the step change of active power does not affect the reactive power. Moreover, there is no over-shoot in the current. As a result, the proposed sliding mode control strategy is robust to parameters' variations with excellent dynamic and steady-state performances.

Table 2. Quantitative comparison of simulation results.

Control method	Transitory response (ms)		THD (%)
	P_p	Q_p	I
PI	41	55	1
SMC	1	2	1.22

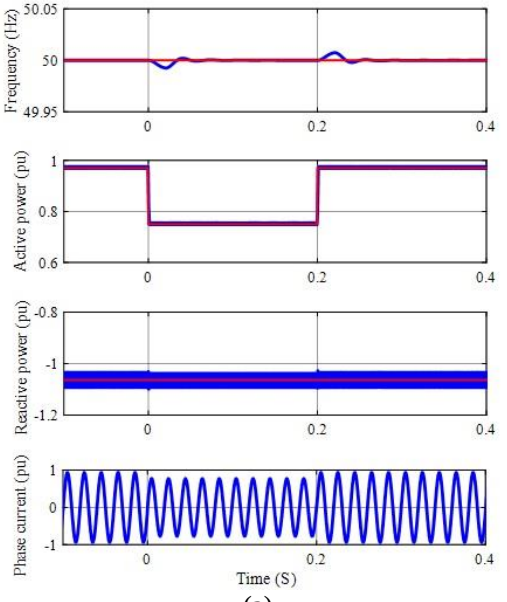

(a)

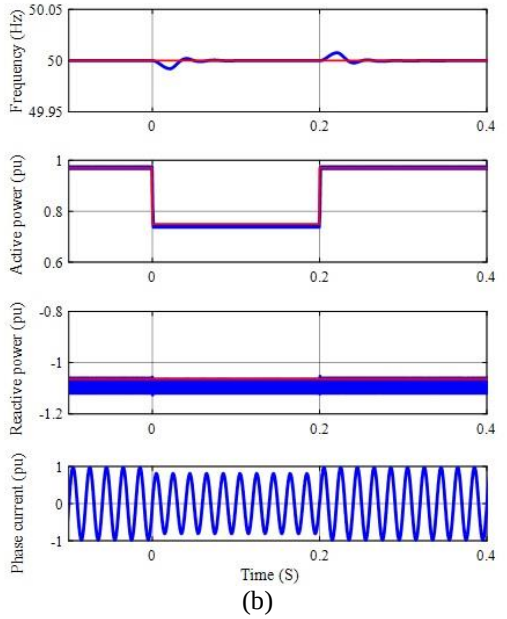

(b)

Fig. 8. Frequency, active and reactive power and phase current: (a) without parameters variations, (b) with 50% variation in resistances.

5. CONCLUSION

To control voltage and frequency in micro-grid with sudden changes in load, a balanced generation should be preserved. In order to regulate voltage and frequency of the micro-grid, sharing and balancing power are critical using a robust control method. To do this**,** an improved sliding mode control of SVPWM switching method for the active generator was proposed to control both frequency and amplitude of voltage. The proposed controller directly determines the required voltage based on the current, voltage, and values of active and reactive powers. The proposed method obtains the voltage in the stationary reference frame, outperforming the PI which is sensitive to the transformation from stationary to synchronous reference-frame. The simulation results are provided and they have shown the robustness and feasibility of the proposed sliding mode control during different operating conditions and system parameter variations. Proposed method controls active and reactive powers or voltage and frequency pairs simultaneously such that voltage stability and frequency stability of power network are promoted. The main features of the proposed control system can be summarized as:

- faster transient response power compared to PI
- ability to control both active and reactive power directly without overshoot and with constant switching frequency
- robustness against the system parameters variation

REFERENCES

[1] X. Tang, K. M. Tsang, and W. L. Chan, **"A Power Quality Compensator with DG Interface Capability using Repetitive Control,"** *IEEE Trans. Energy. Convers.*, Vol. 27, No. 2, pp. 213-219, 2012.

[2] J. Guerrero, P. C. Loh, T. L. Lee, and M. Chandorkar, **"Advanced Control Architectures for Intelligent Microgrids-Part II: Power Quality, Energy Storage, and AC/DC Microgrids,"** *IEEE Trans. Ind. Electron*., Vol. 60, No. 4, pp. 1263-70, 2013.

[3] R. Kadri, J. P. Gaubert, and G. Champenois, **"An Improved Maximum Power Point Tracking for Photovoltaic Grid-Connected Inverter based on Voltage-Oriented Control,"** *IEEE Trans. Ind. Electron.*, Vol. 58, No. 1, pp. 66-75, 2011.

[4] M. P. Kazmierkowski and L. Malesani, **"Current Control Techniques for Three-Phase Voltage Source PWM Converters: a Survey,"** *IEEE Trans. Ind. Electron.*, Vol. 45, No. 5, pp. 691-703, 1998.

[5] J. Hu, J. Zhu, D. G. Dorrell, and J. M. Guerrero, **"Virtual Flux Droop Method, a New Control Strategy of Inverters in Micro-grids,"** *IEEE Trans. Power Electron.*, Vol. 29, No. 9, pp. 4704-11, 2014.

[6] C. T. Pan and L. Yihung, **"Modeling and Control of Circulating Currents for Parallel Three-Phase Boost Rectifiers with Different Load Sharing,"** *IEEE Trans. Ind. Electron.*, Vol. 55, No. 4, pp. 2776-85, 2008,

[7] Z. Zeng, H. Li, S. Tang, H. Yang, and R. Zhao, **"Multi-objective Control of Multifunctional Grid-Connected Inverter for Renewable Energy**

Integration and Power Quality Service," *IET Power Electron.*, Vol. 9, No. 4, pp. 761-70, 2016.

[8] E. Limouchi, S. A Taher, and B. Ganji, **"Active Generators Power Dispatching Control in Smart Grid,"** 21st Conference on Electrical Power Distribution Networks Conference (EPDC), Karaj, Iran, pp 26-32, 2016

[9] S. Peng, A. Luo, Y. Chen, and Z. Lv, **"Dual-loop Power Control for Single Phase Grid-Connected Converters with LCL Filter,"** *J. Power Electron.*, Vol. 11, No. 4, pp. 1-8, 2011.

[10] M. Sitbon, S. Schacham, and A. Kuperman, **"Disturbance Observer Based Voltage Regulation of Current-Mode-Boost-Converter Interfaced Photovoltaic Generator,"** *IEEE Trans. Ind. Electron.*, Vol. 62, No. 9, pp. 5776–5785, 2015.

[11] A. G. Yepes, F. D. Freijedo, J. Doval-Gandoy, O. Lopez, J. Malvar, and P. Fernandez -Comesana, **"Effects of Discretization methods on the Performance of Resonant Controllers,"** *IEEE Trans. Power Electron.*, Vol. 25, No. 7, pp. 1692-1712, 2010.

[12] B. Kuperman, **"Proportional-Resonant Current Controllers design based on Desired Transient Performance,"** *IEEE Trans. Power Electron.*, Vol. 30, No. 10, pp. 5341-45, 2015.

[13] A. Kannana, N. K. Mohantyb, and R. Selvarasuc, **"A New Topology for Cascaded H-bridge Multilevel Inverter with PI and Fuzzy Control,"** *Energy Procedia*, Vol. 117, pp. 917-26, 2017.

[14] F. Karbakhsh, G. B. Gharehpetian, J. Milimonfared, and A. Teymoori, **"Three-phase Photovoltaic Grid-Tied Inverter based on Feed-Forward Decoupling Control using fuzzy-PI Controller,"** 7th Power Electronics, Drive Systems & Technologies Conference (PEDSTC) , Tehran, Iran, pp. 16-18, 2016.

[15] K. Sinthipsomboon,W. Pongaen and P. Pratumsuwan, **"A Hybrid of Fuzzy and Fuzzy Self-tuning PID Controller for Servo Electro-hydraulic System,"** 6th IEEE Conference on Industrial Electronics and Applications, Beijing, China, pp. 220-25, 2011.

[16] P. Cortes, J. Rodriguez, C. Silva, and A. Flores, **"Delay Compensation in Model Predictive Current Control of a Three-Phase Inverter,"** *IEEE Trans. Ind. Electron.*, Vol. 59, No. 2, pp. 1323-25, 2012.

[17] M. Datta, T. Senjyu, A. Yona, T. Funabashi, and C. H. Kim, **"A Frequency Control Approach By Photovoltaic Generator in a PV-Diesel Hybrid Power System,"** *IEEE Trans. Energy. Convers.*, Vol. 26, No. 2, pp. 559-71, 2011.

[18] M. N. Marwali and A. Keyhani, **"Control of Distributed Generation System-Part I: Voltages and Currents Control,"** *IEEE Trans. Power Electron.*, Vol. 19, No. 6, pp. 1541-50, 2004.

[19] G. Bartolini, A. Ferrara, and E. Usai, **"Chattering Avoidance by Second Order Sliding Mode Control,"** *IEEE Trans. Automat. Control*, Vol. 43, No. 2, pp. 241-46, 1998.

[20] G. P. Incremona, M. Cucuzzella, and A. Ferrara, **"Adaptive Suboptimal Second-Order Sliding Mode Control for Micro Grids,"** *International Journal of Control*, pp. 1-19, 2016.

[21] M. Cucuzzella, R. Lazzari, T. Trip, S. Rosti, and C. Sandroni, **"Sliding Mode Voltage Control of Boost Converters in DC Microgrids",** *Control Engineering Practice*, Vol. 73, pp. 161-170, 2018

[22] Y. Mi, H. Zhang, Y. Fu, Ch. Wang, P. Ch. Loh, and P. Wang, **"Intelligent Power Sharing of DC Isolated Microgrid Based on Fuzzy Sliding Mode Droop Control"**, *IEEE Trans. Smart Grid*, Vol. 10, No. 3, pp. 2396-2406, 2019

[23] J. C. Vasquez, J. M. Guerrero, A. Luna, P. Rodriguez, and R. Teodorescu, **"Adaptive Droop Control Applied to Voltage Source Inverters Operating in Grid-Connected and Islanded Modes,"** *IEEE Trans. Ind. Electron.*, Vol. 56, No. 10, pp. 4088-96, 2009.

[24] T. Wu, Z. Liu, J. Liu, S. Wang, Z. You, **"A Unified Virtual Power Decoupling Method for Droop-Controlled Parallel Inverters in Micro-Grids,"** *IEEE Trans. Power Electron.*, Vol. 31, No. 8, pp. 5587-5603, 2016.

[25] L. Collins and J. K. Ward, **"Real and Reactive Power Control of Distributed PV Inverters for Overvoltage Prevention and Increased Renewable Generation Hosting Capacity,"** *Renewable Energy*, Vol. 81, pp. 464-71, 2015.

[26] N. Kumar, T. K. Saha, and J. Dey, **"Modeling, Control and Analysis of Cascaded Inverter Based Grid-Connected Photovoltaic System,"** *International Journal of Electrical Power & Energy Systems*, Vol. 78, pp. 165-73, 2016.

[27] E. Bianconi and et al., **"A Fast Current-based MPPT Technique Employing Sliding Mode Control,"** *IEEE Trans. Ind. Electron.*, Vol. 60, No., pp. 1168-78, 2013.

[28] A. Nilsson, A. Sannino, **"Efficiency Analysis of Low- And Medium Voltage dc Distribution Systems,"** IEEE PES General Meeting, Washington DC, USA, Vol. 2, pp. 2315-21, 2004.

[29] J. N. Edward, A. Ramadan, and E. Shatshat, **"Multi-Microgrid Control Systems,"** IEEE PES General Meeting, Providence, RI, USA, pp. 1-6, 2010.